

Research Article

DY131 activates ERR γ /TFAM axis to protect against metabolic disorders and acute kidney injury

 Wei Gong^{1,2,3,*}, Lingling Lu^{1,2,3,*}, Haoyang Ma^{4,*}, Mingfeng Shan^{1,2,3}, Xinwen Fan^{1,2,3}, Mi Bai^{1,2,3}, Yue Zhang^{1,2,3}, Songming Huang^{1,2,3},  Zhanjun Jia^{1,2,3} and Aihua Zhang^{1,2,3}

¹Department of Nephrology, Children's Hospital of Nanjing Medical University, Nanjing, China; ²Nanjing Key Laboratory of Pediatrics, Children's Hospital of Nanjing Medical University, Nanjing, China; ³Jiangsu Key Laboratory of Pediatrics, Nanjing Medical University, Nanjing, China; ⁴Department of Geriatrics, The Second Affiliated Hospital, School of Medicine, Zhejiang University, Zhejiang, China

Correspondence: Aihua Zhang (zhaihua@njmu.edu.cn) or Zhanjun Jia (jiazj72@hotmail.com) or Songming Huang (smhuang@njmu.edu.cn)

Renal tubular injury is considered as the main pathological feature of acute kidney injury (AKI), and mitochondrial dysfunction in renal tubular cells is implicated in the pathogenesis of AKI. The estrogen-related receptor γ (ERR γ) is a member of orphan nuclear receptors which plays a regulatory role in mitochondrial biosynthesis, energy metabolism and many metabolic pathways. Online datasets showed a dominant expression of ERR γ in renal tubules, but the role of ERR γ in AKI is still unknown. In the present study, we investigated the role of ERR γ in the pathogenesis of AKI and the therapeutic efficacy of ERR γ agonist DY131 in several murine models of AKI. ERR γ expression was reduced in kidneys of AKI patients and AKI murine models along with a negative correlation to the severity of AKI. Consistently, silencing ERR γ *in vitro* enhanced cisplatin-induced tubular cells apoptosis, while ERR γ overexpression *in vivo* utilizing hydrodynamic-based tail vein plasmid delivery approach alleviated cisplatin-induced AKI. ERR γ agonist DY131 could enhance the transcriptional activity of ERR γ and ameliorate AKI in various murine models. Moreover, DY131 attenuated the mitochondrial dysfunction of renal tubular cells and metabolic disorders of kidneys in AKI, and promoted the expression of the mitochondrial transcriptional factor A (TFAM). Further investigation showed that TFAM could be a target gene of ERR γ and DY131 might ameliorate AKI by enhancing ERR γ -mediated TFAM expression protecting mitochondria. These findings highlighted the protective effect of DY131 on AKI, thus providing a promising therapeutic strategy for AKI.

Introduction

Acute kidney injury (AKI) is a complex clinical syndrome manifesting in response to diverse causative factors and emerging as a pressing global public health concern due to its escalating morbidity and mortality rates [1,2]. Annually, more than 13 million individuals succumb to AKI, resulting in 1.7 million deaths worldwide, with an alarming 24% mortality rate observed in hospital settings [2,3]. Moreover, survivors face an elevated risk of progressing to chronic kidney disease (CKD), imposing a substantial societal burden due to the enduring repercussions of the disease [3]. Despite the profound impact of AKI on public health, there are still limited treatment strategies in clinic.

The cause of AKI encompasses a spectrum of instigators, including ischemic/reperfusion, nephrotoxicity, and obstruction, with a common result for inflicting damage upon renal proximal tubules [4]. Unraveling the pathogenic mechanisms underlying AKI becomes imperative to protect renal proximal tubules against these multifaceted insults. Renal proximal tubular cells, rich in mitochondria crucial for sustaining constant ATP production, play a pivotal role in maintaining cellular functions [5]. Recent investigations highlight disruptions in mitochondrial function and metabolism as primary culprits for tubular cell injury,

*These authors contributed equally to this work.

Received: 06 February 2024

Revised: 22 May 2024

Accepted: 11 June 2024

Accepted Manuscript online:
11 June 2024

Version of Record published:
21 June 2024

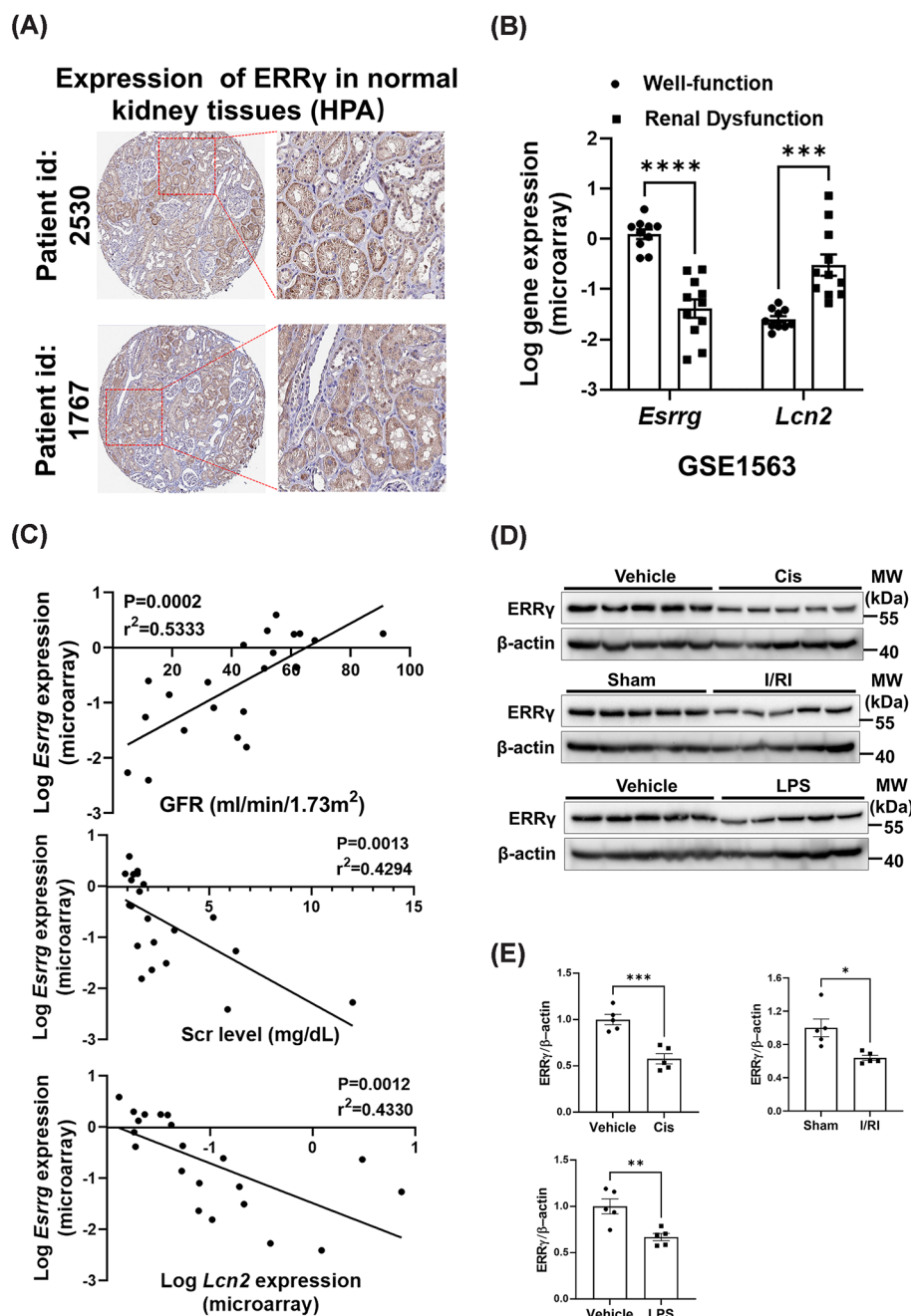


Figure 1. ERR γ expression in AKI patients and murine models

(A) Representative micrographs of immunohistochemical staining of ERR γ in human normal kidney tissues from HPA datasets (<https://www.proteinatlas.org>, HPA044678, [35]). (B) Expression microarray analysis of kidney biopsies identified a decreased expression of *Esrrg* in patients with renal dysfunction ($n=11$) compared with well-functional group ($n=10$). (C) Pearson correlation analysis of *Esrrg* level and glomerular filtration rates (GFR, $n=21$), serum creatinine (Scr, $n=21$) levels and *Lcn2* levels ($n=21$), respectively. Data were extracted and analyzed from GSE1563 in GEO datasets and Nephroseq. (D) Immunoblot of ERR γ in kidneys after cisplatin injection, unilateral I/R operation and LPS challenge. (E) Semiquantification of ERR γ ($n=5$ per group). Data are presented as mean \pm SEM. * $P<0.05$, ** $P<0.01$, *** $P<0.001$, **** $P<0.0001$.

whereby damaged mitochondria not only compromise ATP supply but also contribute to the amplification of injury, cell death, and inflammation [6–8]. Strategies aimed at preserving normal mitochondrial function and metabolism emerge as promising avenues for mitigating AKI [9,10].

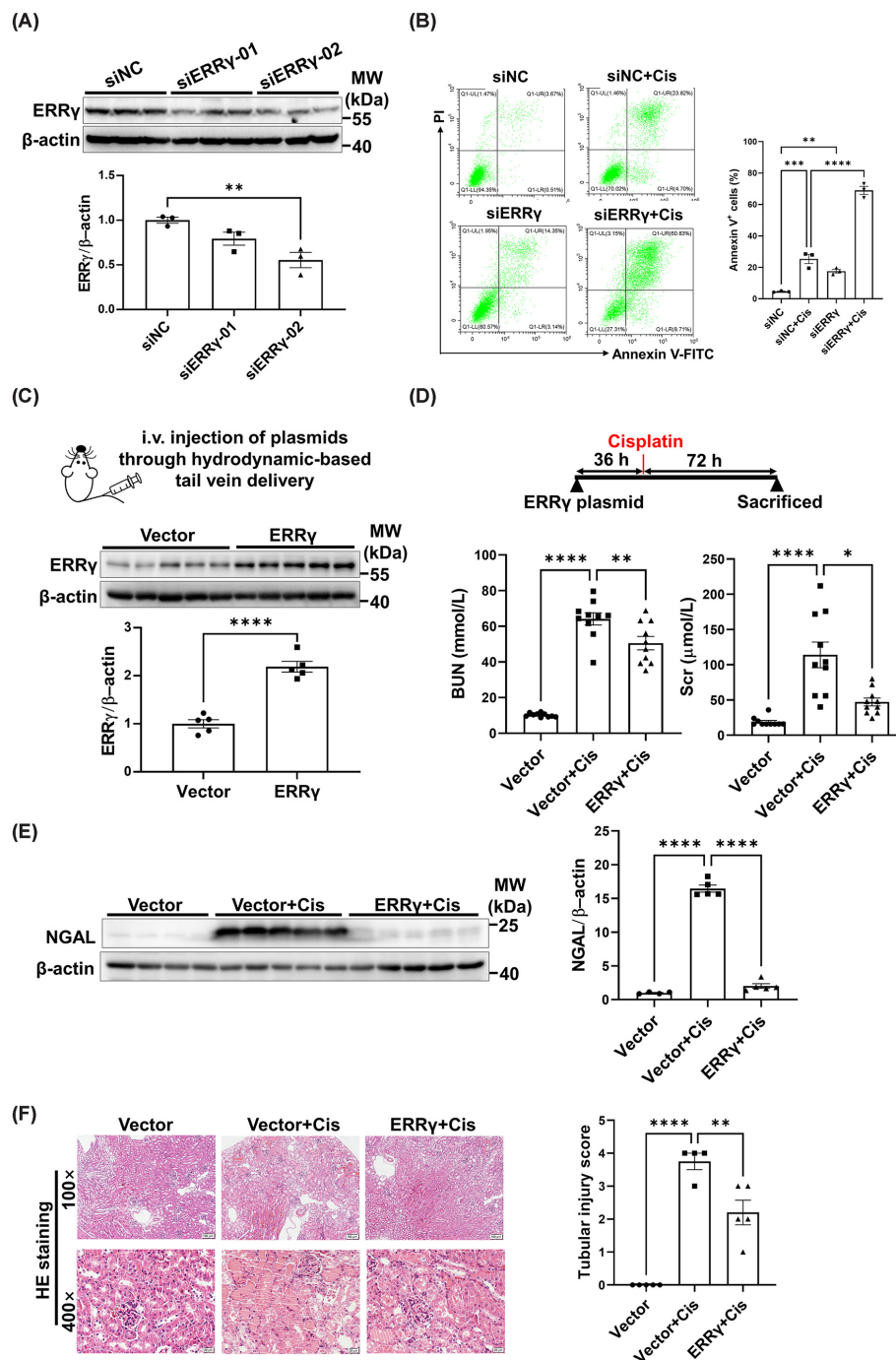


Figure 2. ERRγ protected against tubular cells injury during AKI

(A) siRNAs for ERRγ were transfected to RTECs to silence ERRγ expression and the efficiency was detected using Western blotting. Immunoblot and semiquantification of ERRγ were displayed ($n = 3$ per group). (B) Apoptotic cells were detected using double staining with FITC-annexin V and PI and the quantitative analysis of apoptotic cells (Annexin V-positive, $n = 3$ per group) was performed. (C) Mice were injected with ERRγ plasmid or control vector through hydrodynamic-based tail vein delivery and the expression of ERRγ was detected using Western blotting. Immunoblot and semiquantification of ERRγ were displayed ($n = 5$ per group). (D) Mice were injected with ERRγ plasmid or control vector 36 h before cisplatin administration and were killed 72 h after cisplatin injection. Serum urea nitrogen (BUN) and Scr were assessed ($n = 10$ per group). (E) Immunoblot and semiquantification of NGAL in kidneys ($n = 4-5$ per group). (F) Representative images of HE staining of kidney tissues (Upper panel: 100×; Lower panel: 400×) and analysis of tubular injury score ($n = 4-5$ per group). Data are presented as mean \pm SEM. * $P < 0.05$, ** $P < 0.01$, *** $P < 0.001$, **** $P < 0.0001$.

The estrogen-related receptor γ (ERR γ), an orphan nuclear hormone receptor belonging to the ERR subfamily, emerges as a pivotal player in diverse cellular processes with a tissue-specific expression pattern, notably in metabolically active organs [11,12]. Operating through ligand-independent transcriptional activity by binding to the ERR response element (ERRE), ERR γ regulates critical cellular functions such as proliferation, differentiation, and invasion [13–16].

Extensive studies reveal the involvement of ERR γ in mitochondrial function, energy utilization, oxidative stress, and metabolism, including the restoration of oxidative metabolic capacity and increased expression of mitochondrial respiratory complex proteins upon ERR γ overexpression [17,18]. Besides, many kinds of metabolic pathways can be regulated by ERR γ through its different target genes [19]. The Human Protein Atlas database analysis displayed a predominant ERR γ expression in renal tubules in the kidney. However, the role of ERR γ as well as the potential impact of ERR γ agonist DY131 in AKI remains unknown. In the present study, using several AKI mice models, we report that activation for ERR γ by its agonist DY131 could ameliorate AKI, providing a proof for DY131 as a promising candidate for future clinical applications.

Materials and methods

Human kidney dataset

The dataset comprising human kidney biopsy samples from kidney transplant patients was obtained from the Gene Expression Omnibus (GEO, GSE1563, [20]). This dataset included samples from transplant patients with well-functioning transplants without rejection and kidneys undergoing acute renal dysfunction with or without rejection [21]. Gene expression profiles for these kidney biopsies were determined through microarray analysis. We analyzed the expression data of ERR γ as well as the renal function data corresponding to patients, including GFR, Scr level and Lcn2 expression using the Nephroseq database (<https://www.nephroseq.org/>).

Animals

Male C57BL/6J mice aged 6–8 weeks were provided by Gempharmatech (Nanjing, China). Mice were bred and maintained in the animal care facility of Nanjing Medical University under specific pathogen-free conditions with standard food and water, following a 12-h light/dark cycle. Surgical procedures and experiments of mice were performed in the animal care facility of Nanjing Medical University in accordance with the ethical guidelines and animal procedures approved by the Nanjing Medical University Institutional Animal Care and Use Committee (IACUC-1809017). At the end of the experiment, mice were euthanized by halothane inhalation, and their serum and kidneys were harvested for further analysis.

AKI mice models

Three distinct AKI models were employed in this study: bilateral renal ischemia/reperfusion, nephrotoxic drug and sepsis-induced AKI. For bilateral renal ischemia/reperfusion injury (I/RI)-induced AKI, mice were generally anesthetized with 2% isoflurane and kept at 37°C using thermostatic blanket. Bilateral renal IR injury was caused by renal pedicle clamping for 28 min, as described before [22]. At 36 h after reperfusion, mice were euthanized and serum and renal tissues were collected. Cisplatin was used as nephrotoxic drug to induce AKI. A single dose of cisplatin at 25 mg/kg by intraperitoneal (i.p.) injection was performed and mice were euthanized 72 h later. Sepsis-induced AKI was established by i.p. injection of a single dose of lipopolysaccharide (LPS) at 10 mg/kg, and mice were killed 24 h later.

High-throughput tail vein plasmid delivery

Global ERR γ overexpression *in vivo* was achieved through a hydrodynamic-based tail vein plasmid delivery approach, as previously described [23–25]. ERR γ overexpressing plasmid (obtained from Nanjing Genebay Biotech, China) and a negative control vector were dissolved in saline before injection. Plasmids (2 ml for each mice) were delivered to the tail vein of mice within 10 s. Subsequently, cisplatin was administered 36 h later to induce AKI.

Pharmaceutical treatment

DY131 (Cat. No. HY-15483, MedChemExpress, Princeton, NJ, U.S.A.) was dissolved in dimethyl sulfoxide (DMSO, Cat. No. D2650, Sigma-Aldrich, U.S.A.) and further diluted with 5% Tween-80. Mice were treated with DY131 at 5 mg/kg via i.p. injection. In different AKI models, DY131 was administered according to the previous studies [26–30]. Mice were killed at the indicated time. For investigating the potential toxic effect of DY131 on organs, another separate

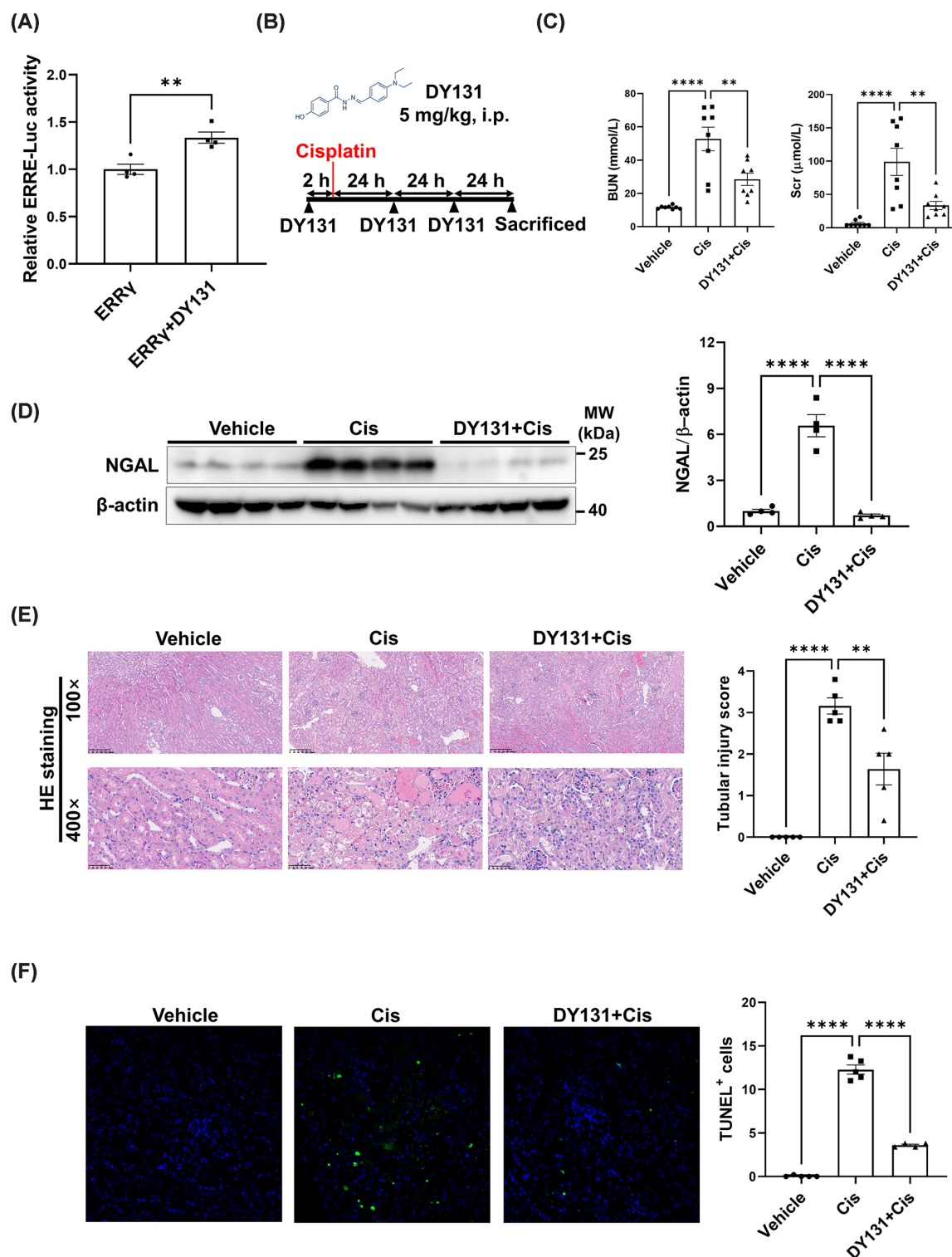


Figure 3. ERRγ agonist DY131 mitigated renal tubular injury in cisplatin-induced AKI

(A) Luciferase reporter assay of 3×ERRE-Luc in RTECs with ERRγ overexpression accompanied by DY131 treatment or not ($n = 4$ per group). (B) Experimental design scheme for administration of DY131 in cisplatin-induced AKI. (C) Serum BUN and Scr were assessed ($n = 8$ per group). (D) Immunoblot and semiquantification of NGAL in kidneys ($n = 4$ per group). (E) Representative images of HE staining of kidney tissues (Upper panel: 100×; Lower panel: 400×) and analysis of tubular injury score ($n = 5$ per group). (F) Representative images of TUNEL staining of kidney sections and analysis of TUNEL-positive cell counts ($n = 4$ –5 per group). Data are presented as mean \pm SEM. ** $P < 0.01$, **** $P < 0.0001$.

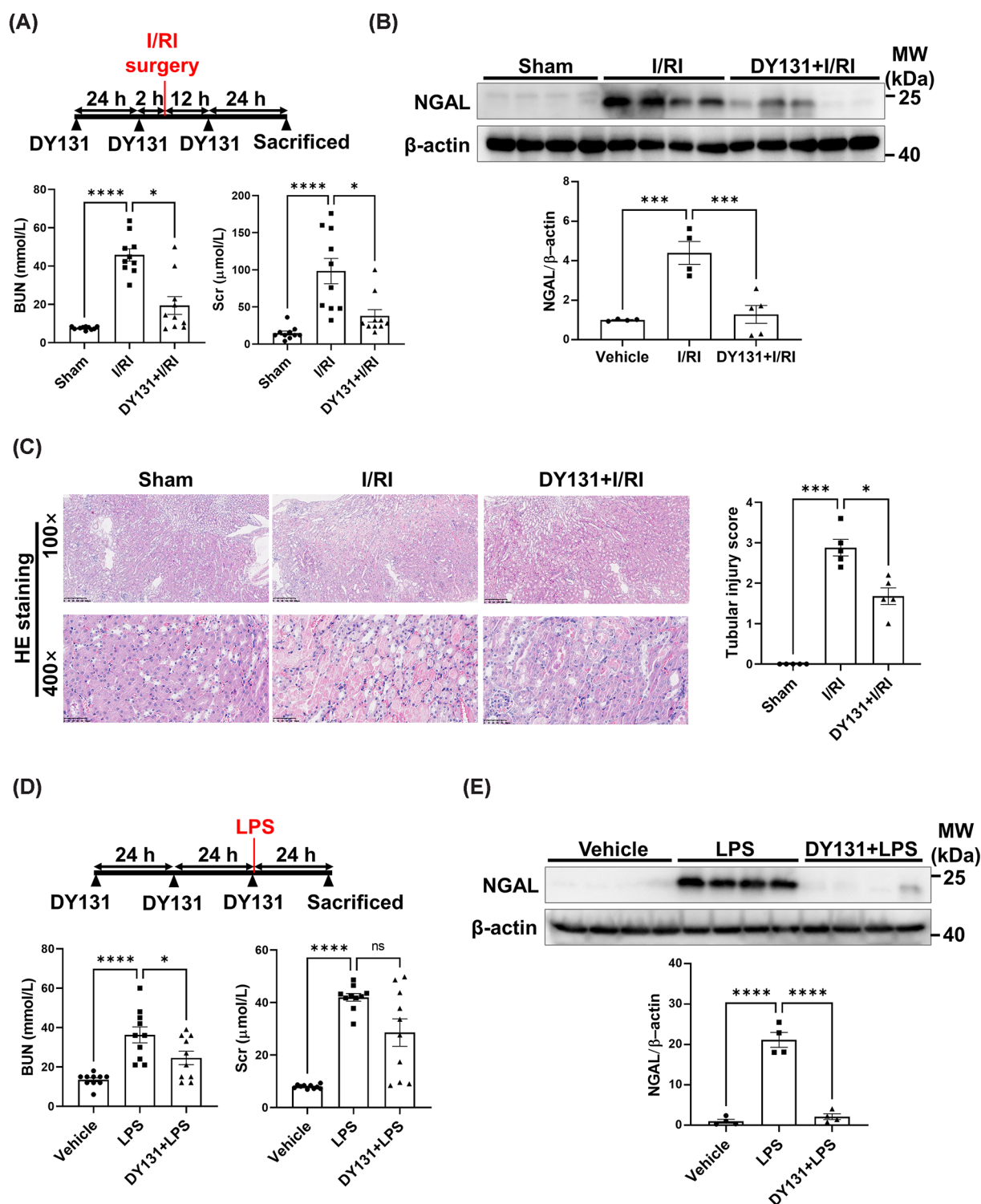


Figure 4. DY131 ameliorated I/IR- and LPS-induced AKI

(A) Experimental design scheme for administration of DY131 in I/RI-induced AKI and serum BUN and Scr were assessed ($n = 10$ per group). (B) Immunoblot and semiquantification of NGAL in kidneys ($n = 4$ –5 per group). (C) Representative images of HE staining of kidney sections (Upper panel: 100 \times ; Lower panel: 400 \times) and analysis of tubular injury score ($n = 5$ per group). (D) Experimental design scheme for administration of DY131 in LPS-induced AKI and serum BUN and Scr were assessed ($n = 10$ per group). (E) Immunoblot and semiquantification of NGAL in kidneys ($n = 4$ per group). Data are presented as mean \pm SEM. * $P < 0.05$, *** $P < 0.001$, **** $P < 0.0001$.

experiment was performed by treating mice with DY131 (5 mg/kg, intraperitoneal injection) or vehicle for three consecutive days and serum samples were collected for assessment of kidney, heart, and liver functions.

Renal, cardiac, and hepatic functions analysis

Blood samples were obtained from the inferior vena cava after mice were euthanized. Serum levels of creatinine (Scr), urea nitrogen (BUN), lactate dehydrogenase (LDH), creatine kinase-MB (CK-MB), aspartate aminotransferase (AST) and alanine aminotransferase (ALT) were detected using a serum biochemical autoanalyzer (Hitachi7600 modular chemistry analyzer, Hitachi Ltd., USA) at Nanjing Children's Hospital.

Histological analysis

Kidney tissues were fixed in 4% paraformaldehyde for 24 h and embedded in paraffin. Hematoxylin–eosin (HE) staining was conducted for histomorphometric analysis of mouse renal tubules as described before [26]. Sections were visualized with microscope and evaluated for tubular injury scores in a blinded fashion on a semiquantitative scale of 0–4. In brief, a pathologist analyzed these sections in a blind manner evaluating renal histopathological changes and scoring by the percentage of renal tubules displaying cell lysis, loss of brush border and cast formation (0, no damage; 1, $\leq 25\%$; 2, 26–50%; 3, 51–75%; 4, $> 75\%$).

TUNEL assay

In situ cell death was determined by TUNEL staining (Cat. No. A112-01/02/03, Vazyme, Nanjing, China) following the manufacturer's instrument. TUNEL-positive signals were imaged using laser scanning confocal microscopy (LSM710, Carl Zeiss, Oberkochen, Germany). The apoptotic cell number in each section was calculated by counting TUNEL-positive apoptotic cells in four-to-five random fields.

Transmission electron microscopy

Renal tissues from mice were quickly dissected and placed in the fixative used in electron microscopy. Tissues underwent standard procedures involving dehydration, osmosis, embedding, sectioning and staining. Mitochondrial structures of renal tubular cells were observed under a transmission electron microscope (JEOL JEM-1010, Tokyo, Japan).

Cell culture and knockdown of $ERR\gamma$ expression *in vitro*

Renal proximal tubular cells of mice (RTECs) were obtained from ATCC (Cat. No. CRL-3361) and cultured following the instructions. $ERR\gamma$ expression was knocked down using small interfering RNA (siRNA) following the manufacturer's instructions. The oligonucleotides designed for $ERR\gamma$ was as follows: si $ERR\gamma$ -01, 5'-GGAGTTACAGTTCAACCAT-3'; si $ERR\gamma$ -02, 5'-GGACGATTCAAGGTAACAT-3'. RTECs were transfected with siRNA for $ERR\gamma$ (si $ERR\gamma$) and the negative control (siNC) respectively using lipofectamine 2000 (Cat. No. 11668019, Invitrogen, Carlsbad, USA) following the manufacturer's instructions.

Flow cytometric cell apoptosis analysis

RTECs were seeded in 12-well plates, incubated 24 h after transfected with si $ERR\gamma$ or siNC, and then treated with cisplatin (5 $\mu\text{g}/\text{ml}$) for additional 12 h. Cells were collected, washed, and resuspended with 100 μl binding buffer. Annexin V-FITC and PI (Annexin V-FITC Apoptosis Detection Kit, Cat. No. 556547, BD Biosciences, San Diego, CA) were added and mixed, followed by incubation in dark at room temperature for 15 min. The rate of Annexin V-positive cells was then detected by flow cytometry (BD Biosciences, San Diego, CA).

Oxygen consumption rate (OCR) measurement

To evaluate the mitochondrial function in RTECs after DY131 treatment, OCR and ATP level were detected, respectively. For details, OCR was measured by XF96 Seahorse analyzer (Seahorse Bioscience, Copenhagen, Denmark) and analyzed as described before [31]. First, RTECs were seeded in a specialized 96-well plate at a density of 3000 cells per well and treated with or without DY131 (0.1 μM). OCR assays were performed followed by the sequential addition of mitochondrial inhibitors including oligomycin, FCCP, rotenone and antimycin A. After assay performance, cells were lysed and the total cellular proteins were quantified by BCA Protein Assay Kit (P0012, Beyotime, Shanghai, China) to correct the final data.

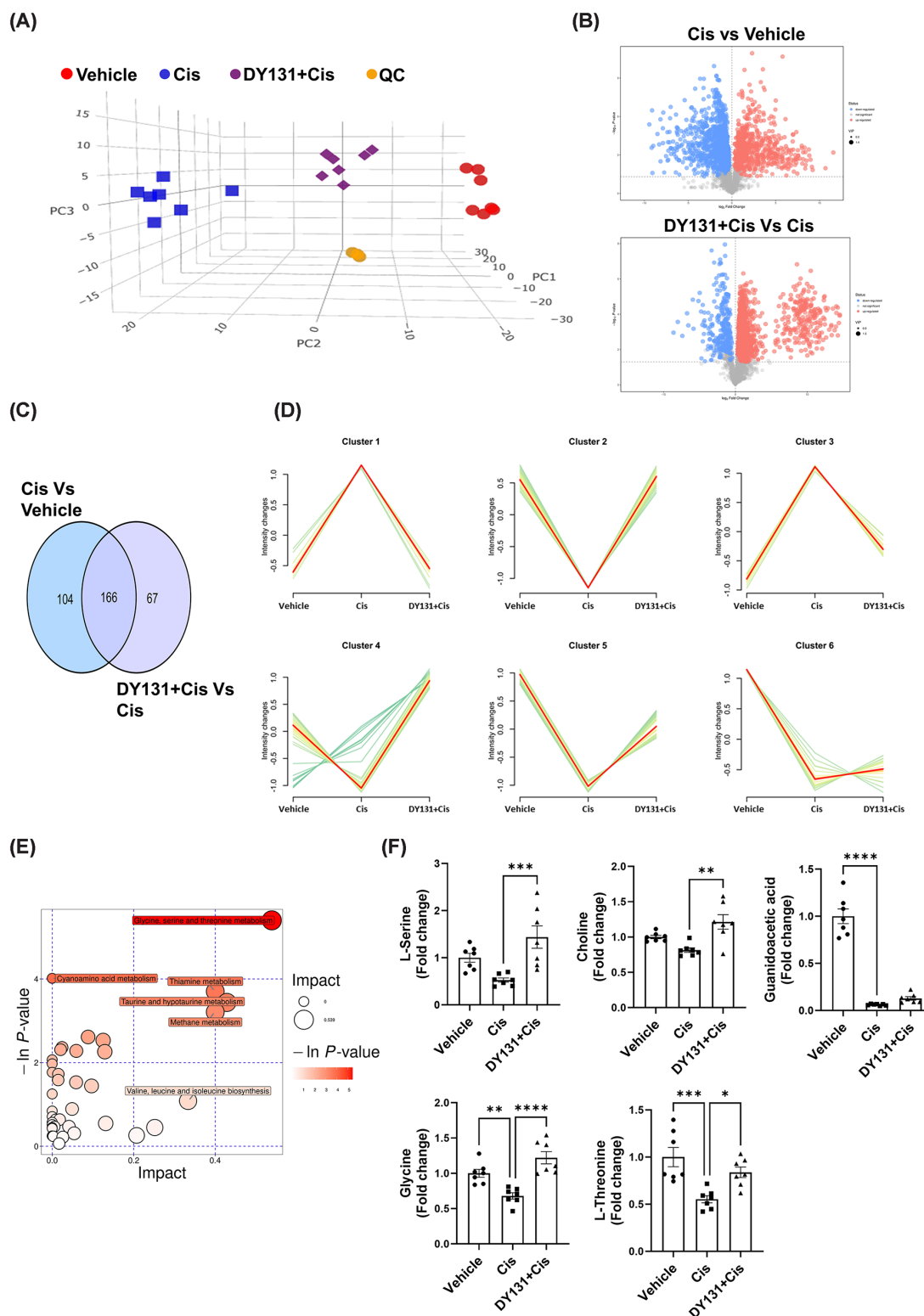


Figure 5. DY131 restored metabolic disorder in cisplatin-induced AKI mice

(A) The scatter plots of PCA model; QC, quality control. (B) Volcano plots showing differentially expressed metabolites (DEMs) in cisplatin vs vehicle group and DY131+cisplatin vs. cisplatin group, respectively. (C) Venn diagram depicting common DEMs in the two comparisons shown in (B). (D) Cluster analysis of change trend for the overlapped DEMs. (E) Metabolic pathways analysis for the overlapped DEMs. (F) Statistical analysis of representative metabolites in the glycine, serine, and threonine metabolic pathways ($n = 7$ per group). Data are presented as mean \pm SEM. * $P < 0.05$, ** $P < 0.01$, *** $P < 0.001$, **** $P < 0.0001$.

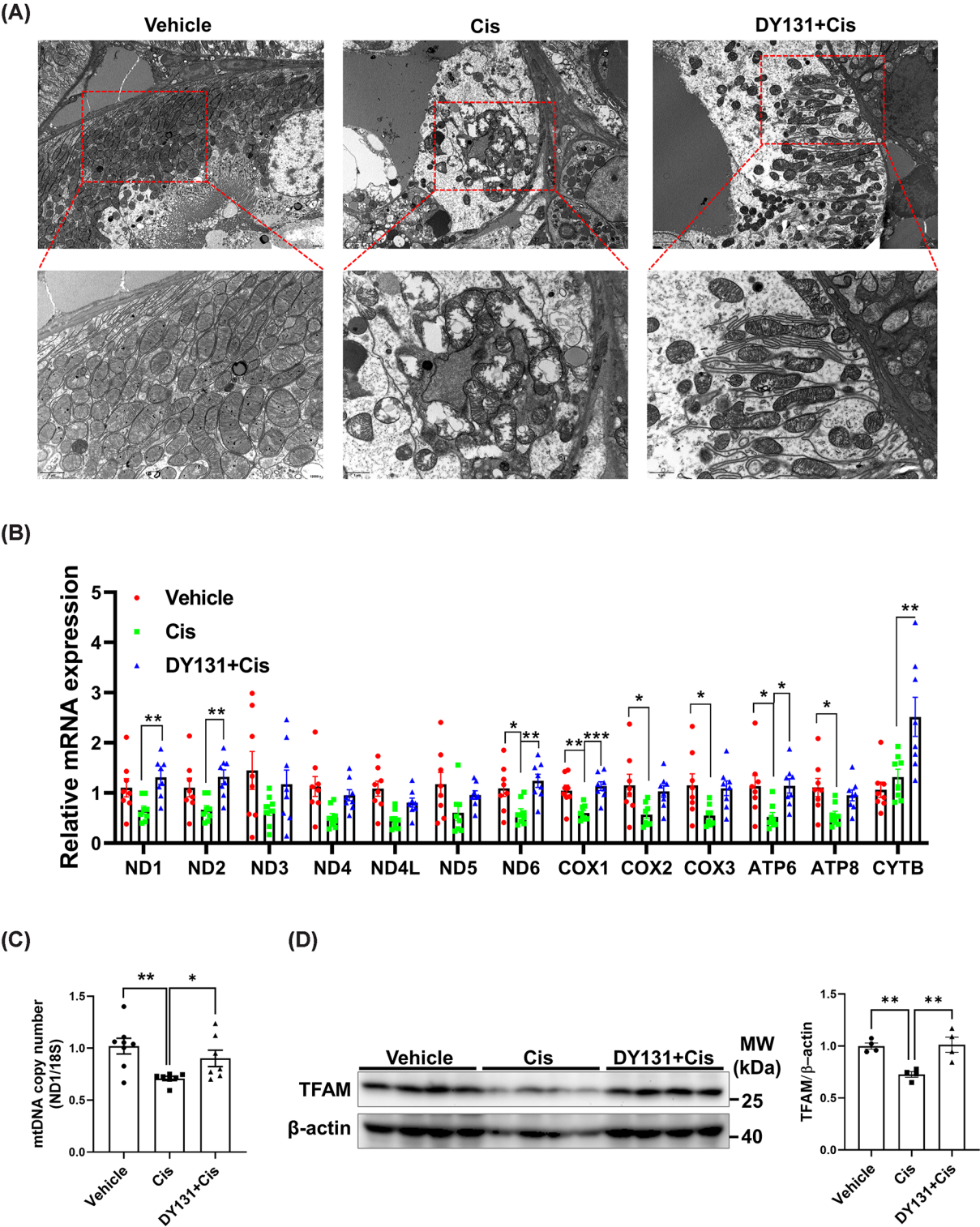


Figure 6. DY131 repaired mitochondrial damage and regulated TFAM expression *in vivo* and *in vitro*
(A) Representative TEM images of proximal renal tubular cells from cisplatin-induced models (Upper panel, scale bar: 2 μ m; Lower panel, scale bar: 2 μ m). (B) The mRNA levels of 13 mitochondria-encoded genes in kidney tissues measured by Q-PCR ($n = 8$ per group). (C) mtDNA content of kidney tissues as assessed by Q-PCR ($n = 7$ –8 per group). (D) Immunoblot and semiquantification of TFAM in kidneys ($n = 4$ per group). Data are presented as mean \pm SEM. * $P < 0.05$, ** $P < 0.01$, *** $P < 0.001$.

Table 1 Primer sequences for Q-PCR

| Gene symbol | Primer sequences (5'-3') | Length | Official full name |
|-------------|--|--------|---|
| mt-Nd1 | F: ACACCTTATTACAACCCAAGAACACAT R: TCATATTATGGCTATGGGTCAGG | 66 bp | NADH dehydrogenase 1, mitochondrial |
| mt-Nd2 | F: CCATCAACTCAATCTCACTTCTATG R: GAATCCTGTTAGTGGTGGAAGG | 104 bp | NADH dehydrogenase 2, mitochondrial |
| mt-Nd3 | F: CCCCAAATAAATCTGTA R: CTCATGGTAGTGGAAGT | 160 bp | NADH dehydrogenase 3, mitochondrial |
| mt-Nd4 | F: GCTTACGCCAACACAGAT R: TAGGCAGAATAGGAGTGAT | 161 bp | NADH dehydrogenase 4, mitochondrial |
| mt-Nd4L | F: GCCATCTACCTTCTTCA R: TAGGGCTAGTCCTACAGC | 229 bp | NADH dehydrogenase 4L, mitochondrial |
| mt-Nd5 | F: GCCAACAACATATTTCAACTTTTC R: ACCATCATCCAATTAGTAGAAAGGA | 76 bp | NADH dehydrogenase 5, mitochondrial |
| mt-Nd6 | F: GGGAGATTGGTTGATGTA R: ATACCCGCAAACAAAGAT | 129 bp | NADH dehydrogenase 6, mitochondrial |
| mt-Cox1 | F: CAGACCGCAACCTAAACACA R: TTCTGGGTGCCCAAGAAT | 95 bp | Cytochrome c oxidase I, mitochondrial |
| mt-Cox2 | F: GCCGACTAAATCAAGCAACA R: CAATGGGCATAAAGCTATGG | 99 bp | Cytochrome c oxidase II, mitochondrial |
| mt-Cox3 | F: CGTGAAGGAACCTACCAAGG R: ATTCCTGTTGGAGGTCAGCA | 176 bp | Cytochrome c oxidase III, mitochondrial |
| mt-Atp6 | F: CCATAAATCTAAGTATAGCCATTCCAC R: AGCTTTTGTAGTTGTGTCGGAAG | 75 bp | ATP synthase 6, mitochondrial |
| mt-Atp8 | F: ACATCCCCTGCGCACC R: GGGGTAATGAATGAGGC | 103 bp | ATP synthase 8, mitochondrial |
| mt-Cytb | F: GAGGTTGGTTCGGTTTTGG R: GTTTTGAAGGGTGGGTGAC | 72 bp | Cytochrome b, mitochondrial |
| mtDNA (ND1) | F: ATCCTCCAGGATTTGGAAT R: ACCGGTAGGAATTGCGATAA | 213 bp | Mitochondrial DNA |
| 18S rRNA | F: TTCGGAACGTAGGCCATGATT R: TTTCGCTCTGGTCCGTCTTG | 101 bp | 18S ribosomal RNA |

ATP level detection

The level of ATP in RTECs was measured by an Enhanced ATP Assay Kit (S0027, Beyotime, Shanghai, China) according to the manufacturer's instructions. RTECs were plated in 96-well plate and treated with or without DY131 (0.1 μ M). After treatment, cells were lysed and the supernatant were obtained for measurement by chemiluminescence with a luminometer plate reader (Promega, Beijing, China). The ATP level was adjusted by the cellular protein concentration quantified by BCA Protein Assay Kit.

Reverse transcription and quantitative real-time PCR (Q-PCR)

Total RNA was extracted from kidneys using Trizol reagent (Cat. No. 9108, Takara Bio, Dalian, China) following the manufacturer's instructions. cDNA was synthesized from 1 μ g RNA using the PrimeScript RT Reagent Kit (Cat. No. RR037A, TaKaRa, Tokyo, Japan). Quantitative real-time PCR (Q-PCR) was performed using the SYBR Green Premix Kit (Cat. No. q111-02/03, Vazyme, Nanjing, China) on the QuantStudio 3 Real-time PCR System (Applied Biosystems, Foster City, CA, U.S.A.). The relative mRNA amount was assessed using the $2^{-\Delta\Delta C_t}$ method, normalized to the level of 18S ribosomal RNA (rRNA). Primer sequences are provided in Table 1.

Mitochondrial genome quantification

Kidney tissues were homogenized into cell suspension and the total DNA was extracted using a DNeasy Tissue Kit (Cat. No. DP304, TIANGEN, Beijing, China). Mitochondrial genome (mtDNA copy number) was determined by Q-PCR. The ratio of mt-DN1 to 18s rRNA represents the relative content of mtDNA.

Western blotting

Kidneys sections or cells were lysed in RIPA buffer (Cat. No. P0013C, Beyotime, Shanghai, China) with 1× protease inhibitor cocktail (Cat. No. 04693132001, Roche, Switzerland) for 30 min on ice. Protein concentration was determined by BCA Protein Assay Kit (Cat. No. P0012, Beyotime, Shanghai, China). Blotting was performed using primary antibodies against ERRγ (Cat. No. sc-393969, SANTA CRUZ, Texas, U.S.A.), β-actin (Cat. No. 66009-1-1g, Proteintech, Wuhan, China), GAPDH (Cat. No. 60004-1-1g, Proteintech, Wuhan, China), NGAL (Cat. No. ab63929, Abcam, Cambridge, U.K.) and TFAM (Cat. No. 22586-1-AP, Proteintech, Wuhan, China).

Luciferase reporter assay

The 3xERRE-luciferase (ERRE-Luc), mice Tfam-promoter-PGL3-Basic (Tfam-Luc) plasmid and pRL-CMV plasmid were ordered from Nanjing Genebay Biotech (Nanjing, China). Mice RTECs were transfected with the Tfam-Luc or ERRE-Luc and co-transfected with ERRγ-expressing plasmid (Genebay Biotech, Nanjing, China) underwent different treatments. Transcriptional activity was determined by the ratio of the reporter plasmid to pRL-TK using Dual-Luciferase Reporter Assay System (Cat. No. E1910, Promega, Beijing, China) according to the manufacture's instruction.

Metabolomics assay

A total of 25 mg of each kidney sample was used for metabolites extraction. Extracts were prepared and analyzed using an LC-MS/MS system (Vanquish, Thermo Fisher Scientific) with a UPLC BEH Amide column (2.1 mm × 100 mm, 1.7 μm) coupled to a Q Exactive HFX mass spectrometer (Orbitrap MS, Thermo) as described before [32]. The quality control (QC) sample was prepared by mixing an equal aliquot of the supernatants from all of the samples.

Raw data were processed with an in-house program based on XCMS, and metabolite annotation was performed using the BiotreeDB MS2 database. The principal component analysis (PCA) was conducted with SIMCA software (V16.0.2, Sartorius Stedim Data Analytics AB, Umea, Sweden). Differentially expressed metabolites (DEMs) were identified based on a Student's *t*-test with a *P*-value < 0.05 and variable importance in the projection (VIP) > 1. Further analysis was performed using the Laboratory Information Management System (LIMS, Biotree, Shanghai, China). The related raw data have been deposited to the metabolomics database Metabolomics Workbench [33].

Statistical analysis

Data were expressed as the mean ± SEM. Student's *t*-test or one-way ANOVA followed by Bonferroni's comparison test was performed to analyze the difference with GraphPad Prism 9. *P*-values of < 0.05 were considered significant.

Results

ERRγ expression in AKI patients and murine models

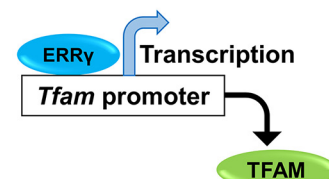
To delineate the role of ERRγ in acute kidney injury (AKI), we initiated our investigation by scrutinizing the gene expression patterns of *Esrrg* in human renal tissue. Immunohistochemical staining from Human Protein Atlas (HPA) database indicated a dominant protein expression in renal tubules of normal kidneys (Figure 1A). Analyzing data from transplant patients with renal dysfunction (GSE1563 [21],) revealed a significant reduction in *Esrrg* (encoding ERRγ) expression in comparison to well-functional kidneys, concurrently with an elevation in *Lcn2* (encoding NGAL, a molecular marker indicative of tubular cell injury [34]) expression (Figure 1B). More importantly, *Esrrg* expression displayed a positive correlation with glomerular filtration rate (GFR) and negative correlations with serum creatinine (Scr) levels and *Lcn2* expression (Figure 1C). Besides, ERRγ expression was detected in several AKI murine models, including bilateral renal I/R, cisplatin and LPS-induced AKI. As shown in Figure 1D,E, ERRγ expression was markedly diminished in kidneys of these experimental AKI models.

ERRγ protected against tubular cell injury during AKI

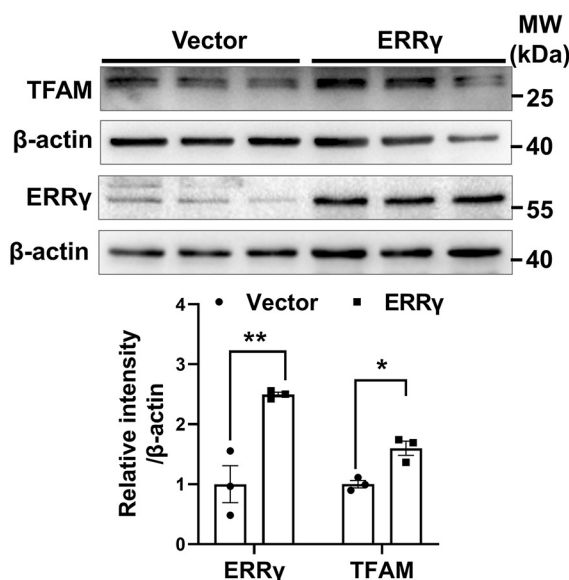
To elucidate the functional implications of ERRγ in renal tubular cell, we knocked down ERRγ in cisplatin-induced renal tubular cells. Figure 2A showed the knockdown efficiency of siERRγ and siERRγ-02 was chosen for further experiments. Attenuated ERRγ expression in renal tubular cells accentuated cisplatin-induced cell apoptosis (Figure 2B). Furthermore, we performed a hydrodynamic gene delivery approach to overexpress ERRγ *in vivo* through hydrodynamic-tail vein-injection of ERRγ plasmid, which has been proved to regulate target gene expression globally, including kidney tissues [24,36,37]. ERRγ expression in kidneys was significantly increased in mice receiving tail vein delivery of ERRγ plasmid (Figure 2C). In mice subjected to cisplatin, ERRγ overexpression was demonstrated to be a

(A)

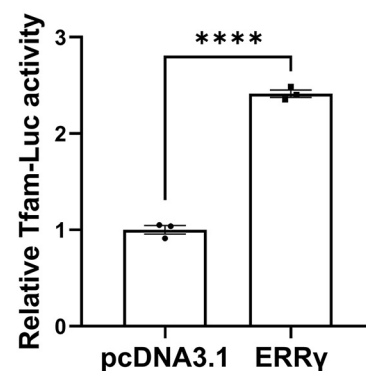
| Name | Score | Relative score | Start | End | Strand | Predicted sequence |
|----------------|----------|----------------|-------|------|--------|--------------------|
| MA0643.1.Esrrg | 10.6416 | 0.912721963 | 172 | 181 | + | CCAAGGGCAA |
| MA0643.1.Esrrg | 6.984178 | 0.858918359 | 932 | 941 | - | TCAATGGCAT |
| MA0643.1.Esrrg | 5.816687 | 0.84174362 | 1418 | 1427 | + | TCAAAGTCAG |
| MA0643.1.Esrrg | 5.362532 | 0.835062634 | 671 | 680 | - | TCCAGGTCAG |
| MA0643.1.Esrrg | 5.318746 | 0.834418506 | 1262 | 1271 | - | GCAAGTTCAA |
| MA0643.1.Esrrg | 5.251152 | 0.833424143 | 694 | 703 | + | GCAAGGATAA |
| MA0643.1.Esrrg | 5.146313 | 0.831881886 | 894 | 903 | - | TCAAGGGCTT |
| MA0643.1.Esrrg | 4.091165 | 0.816359808 | 343 | 352 | + | TGAAGGAGAC |
| MA0643.1.Esrrg | 4.089893 | 0.816341092 | 1172 | 1181 | + | AGAAGATCAA |
| MA0643.1.Esrrg | 3.799398 | 0.812067682 | 623 | 632 | + | TAAATGTTAT |
| MA0643.1.Esrrg | 3.67523 | 0.810241072 | 990 | 999 | + | TGTAGGACAC |
| MA0643.1.Esrrg | 3.630487 | 0.809582855 | 1729 | 1738 | + | CGAAGCTCAG |
| MA0643.1.Esrrg | 3.486027 | 0.807457743 | 1412 | 1421 | + | TGTATGTCAA |



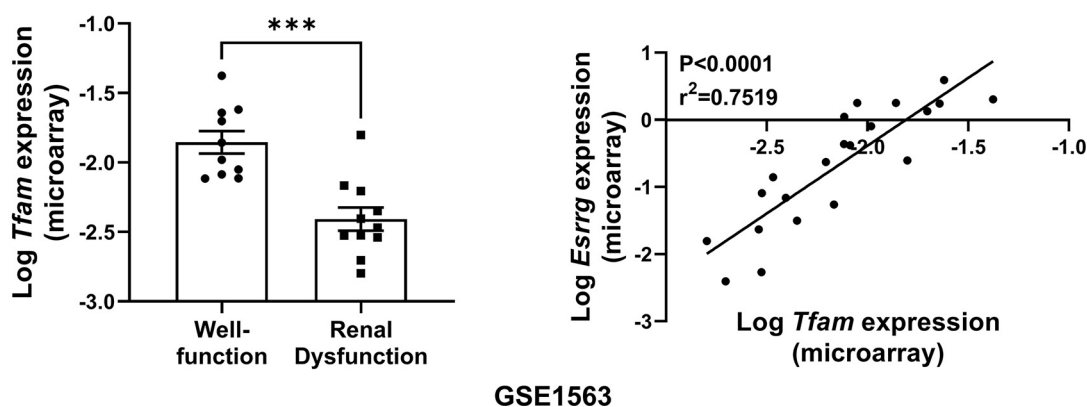
(B)



(C)



(D)



GSE1563

Figure 7. ERRγ regulated the expression of TFAM

(A) Putative ERRγ binding sites predicted by JASPAR within the promoter region of *Tfam* and the schematic diagram. (B) RTECs were transfected with ERRγ plasmid and the immunoblot and semiquantification of TFAM and ERRγ were shown ($n = 3$ per group). (C) Dual-Luciferase Reporter Assay ($n = 3$ per group). (D) Decreased expression of *Tfam* in patients with renal dysfunction ($n = 11$) compared with well-functional group ($n = 10$), and correlation analysis of *Esrrg* and *Tfam* expression was performed ($n = 21$). Data were extracted from GSE1563. Data are presented as mean \pm SEM. * $P < 0.05$, ** $P < 0.01$, *** $P < 0.001$, **** $P < 0.0001$.

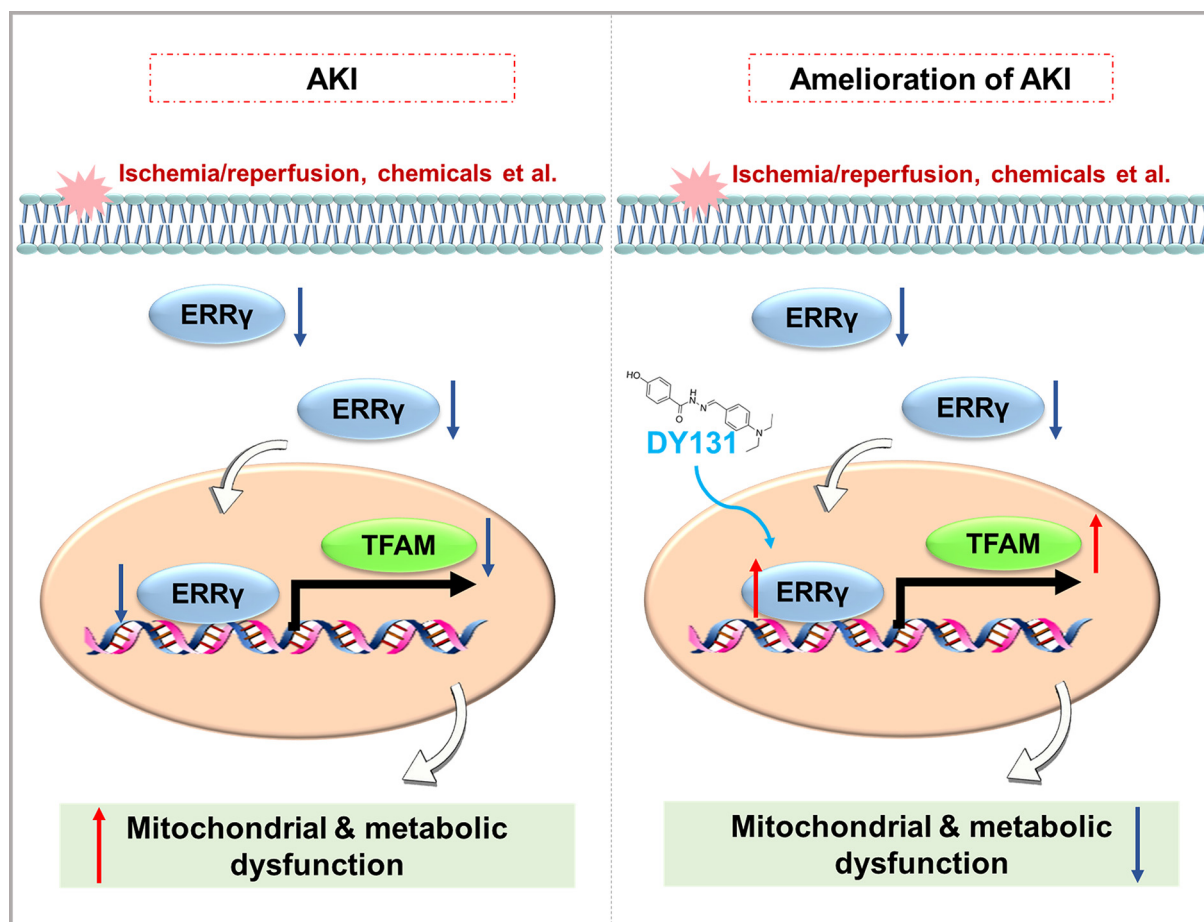


Figure 8. Schematic diagram illustrating the renoprotective role of $ERR\gamma$ and DY131 in AKI

DY131, which led to the transcriptional activity of $ERR\gamma$, could increase the expression of TFAM, accordingly promoting the mitochondrial function maintenance and metabolic homeostasis, and thus inhibiting renal tubular injury in AKI.

renoprotective role in kidneys, as evidenced by reduced BUN, Scr levels, and NGAL expression (Figure 2D,E). Pathological staining and image analysis displayed ameliorated pathological injury by $ERR\gamma$ overexpression, including the tubular brush border loss, tubular dilatation and cast formation in kidneys (Figure 2F).

$ERR\gamma$ agonist DY131 mitigated renal tubular injury in various mice models of AKI

Building upon the protective role of $ERR\gamma$ in AKI, we investigated the therapeutic potential of DY131, an $ERR\gamma$ agonist with preferential selectivity for $ERR\gamma$ [38]. $ERR\gamma$ transcriptional activity in renal tubular cells was assessed by a cell-based reporter assay using co-transfecting with $ERR\gamma$ -expressing plasmid and a luciferase reporter construct driven by three ERR response elements ($3 \times ERRE$ -Luc [38–40]). Increased luciferase activity of the reporter genes was observed in renal tubular cells with DY131 treatment (Figure 3A), suggesting that DY131 could modulate the transcriptional activity of $ERR\gamma$ in renal tubular cells. Next, we detect the effect of DY131 in AKI mice. Pretreatment of DY131 before cisplatin challenge followed by treating daily in cisplatin-induced AKI mice (Figure 3B) yielded significant reductions in BUN and Scr levels, accompanied by decreased NGAL expression, diminished tubular injury, and a decrease in apoptotic cell numbers (Figure 3C–F). Besides, the therapeutic effect of DY131 in cisplatin-induced AKI was investigated. Therapeutic administration of DY131 after cisplatin treatment also significantly attenuated kidney injury as well as improving heart function (Supplementary Figure S1).

To confirm these findings in separate models of AKI, two additional mice models were employed, I/R and LPS-induced AKI. Kidneys from mice subjected to I/R exhibited elevated levels of BUN, Scr, tubular injury markers and conspicuous pathological damage to renal tubules, while administration of DY131 demonstrated a significant

amelioration of these pathological indicators (Figure 4A–C). A comparable trend was observed in the LPS-induced AKI model (Figure 4D,E). These data further substantiated DY131's therapeutic efficacy in different pathophysiology of AKI.

Of notes, the current dose of DY131 used in mice experiments had no significant toxic effect on the functions of kidney, heart, and liver (Supplementary Figure S2), suggesting an effective and safe dosage used in the mice models.

DY131 restored metabolic disorder in cisplatin-induced AKI mice

Given the integral role of metabolic dysfunction in AKI pathogenesis [41], we conducted non-targeted metabolomics to assess DY131's impact on renal metabolism during AKI. The principal component analysis (PCA) score plots showed that the three groups had good reproducibility and separation (Figure 5A). Significantly altered metabolites between cisplatin versus vehicle groups and DY131+cisplatin versus cisplatin groups were identified (P -value < 0.05 and VIP > 1, Figure 5B). Overall, we identified 270 and 233 differentially expressed metabolites (DEMs) in these two comparisons respectively and a total of 166 DEMs were overlapped (Figure 5C). Subsequent analysis revealed that a total of 166 DEMs were overlapped and could be categorized into six distinct clusters. Notably, clusters 1 and 3 encompassed DEMs that displayed a substantial increase in the cisplatin-treated group, while to be restored to near-normal levels following DY131 intervention. Conversely, DEMs in clusters 2, 4, 5, and 6 exhibited marked decreases in the cisplatin-exposed group but demonstrated a significant recovery upon DY131 treatment (Figure 5D). These analyses revealed significant alterations in metabolites during AKI, with DY131 treatment partially reversing the disturbed metabolism in AKI. Meanwhile, pathway analysis indicated an enrichment in amino acid metabolic pathways, particularly in the glycine, serine, and threonine metabolism (Figure 5E), and the levels of representative metabolites, such as L-serine, choline, guanidoacetic acid, glycine and L-threonine were up-regulated in DY131-treated group (Figure 5F).

DY131 repaired mitochondrial damage through promoting TFAM expression

Mitochondrial damage and dysfunction play an important role in the pathogenesis of AKI and closely associated with metabolic disorders [42]. We assessed whether DY131 treatment reduced the mitochondrial damage induced by cisplatin. Renal ultrastructure by electron microscopy in cisplatin group showed abnormal mitochondria with evident mitochondrial swelling and vacuolation and cristae destruction in renal tubular cells. However, administration with DY131 mitigated these abnormalities (Figure 6A). Furthermore, *in vitro* experiments were performed to illustrate the impact of DY131 on mitochondrial function. Consistently, DY131 significantly up-regulated the oxygen consumption rate (OCR) of RTECs, especially in the ATP-linked respiration, and enhanced the ATP production in RTECs (Supplementary Figure S3). Concurrently, DY131 treatment improved the transcriptional activity of mitochondrial genes and increased mitochondrial gene copy numbers, indicating an enhanced mitochondrial biogenesis *in vivo* (Figure 6B,C). Since mitochondrial transcriptional factor A (TFAM) plays a key role in the biosynthesis of mtDNA and mitochondrial function maintenance, and genetic restoration of TFAM attenuated mitochondrial dysfunction and cell injury induced by cisplatin [43], we further examined the expression of TFAM in DY131-treated mice and found a trend of increased expression (Figure 6D), suggesting its potential role in DY131-mediated mitochondrial repair.

As ERR γ is a key transcriptional factor, we next investigated whether ERR γ could induce TFAM expression. Online JASPAR prediction tool [44] showed that ERR γ could bind to the promoter region of TFAM with 13 possible binding sites, indicating that ERR γ might promote the transcription of TFAM (Figure 7A). To confirm this prediction, overexpression of ERR γ was achieved in renal tubular cells which displayed an up-regulated expression of TFAM (Figure 7B). The data of dual-luciferase reporter assay gave a direct evidence that ERR γ overexpression promoted the transcriptional activity of TFAM promoter (Figure 7C). Besides, we detected the *Tfam* expression in the public datasets of patients with dysfunctional kidneys (GSE1563) and found that *Tfam* expression was significant decreased in renal dysfunction group compared with the well-functional kidneys, and was positively correlated with *Esrrg* expression (Figure 7D). These results collectively indicated that DY131 was effective in treating AKI through the ERR γ -TFAM axis to mitigate mitochondrial damage and metabolic disorders.

Discussion

AKI manifests as a severe injury to kidney tubules, often arising from IR, sepsis, or nephrotoxins. Emerging evidence indicated the pivotal role of mitochondrial dysfunction in AKI pathogenesis. Notably, mitochondrial pathologic changes precede detectable kidney dysfunction and persist in non-recovering tubules, as illustrated by an AKI

mouse model induced by glycerol, revealing marked ultrastructural alterations occurring even before kidney injury onset. Furthermore, genetic or pharmacological interventions preventing mitochondrial dysfunction have proven effective in protecting against AKI and mitigating its progression to CKD [42,45]. Injured mitochondria not only compromise cellular ATP production but also serve as potent sources of molecules amplifying injury, precipitating cell death and inciting inflammation [46]. Therefore, strategies targeting mitochondrial dysfunction or enhancing mitochondrial regeneration emerge as promising therapeutic avenues for AKI.

ERR γ , a member of the orphan nuclear receptor family, is implicated in a spectrum of physiological and pathological processes, particularly within high metabolic demand tissues such as stomach, kidney, and brain [47]. Studies suggested ERR γ has a pivotal role in mitochondrial function, with contributions to metabolic maturation in pancreatic β cells and mitigation of muscle damage [48,49]. In the renal context, ERR γ is predominantly expressed in renal tubules, playing a role in ciliary dynamics [50]. Public datasets reveal a significant decrease in ERR γ expression in patients with renal dysfunction, indicating potential involvement in AKI severity. However, the precise role of ERR γ in renal tubular injury and the impact of its agonist remain unclear. In the present study, we found that ERR γ overexpression *in vivo* ameliorated renal dysfunction and pathology induced by cisplatin, suggesting a renoprotective role of ERR γ in AKI. Furthermore, knocking-down ERR γ expression in renal tubular cells accentuated cisplatin-induced cell apoptosis *in vitro*, even induced apoptotic death without cisplatin challenge. ERR γ is highly expressed in tissues with high energy demands and demonstrated to play a vital role in mitochondrial oxidative functions, cellular bioenergetics and metabolism [17,51,52]. Our results also displayed that activating ERR γ by its agonist protected against mitochondrial damage and metabolic disorder in kidney. Therefore, knockdown of ERR γ might induce cell death due to mitochondrial dysfunction. Consistently, other studies found that mitochondrial dysfunction and cell death/tissues injury occurred because of ERR γ deletion in acinar cells, neuronal cells, prostate cancer and so on [19,51,53].

The ERR γ -specific agonist, DY131, emerges as a selective and promising modulator, demonstrating effective in various pathological conditions [13,38]. DY131 treatment inhibited the generation of osteoclast and further protested against inflammatory bone loss [54]. In LPS-induced acute liver injury, DY131 could ameliorate liver inflammation and restore liver function [27]. Besides, DY131 prevented the abnormal cell turnover in hypoxia-treated placentas by inducing ERR γ signaling pathways [55]. Intriguingly, our study reveals that DY131, administered via intraperitoneal injection, ameliorates renal function and tubular injury in AKI induced by cisplatin, I/RI, and LPS. Importantly, DY131 alleviated cisplatin-induced mitochondrial dysfunction and metabolic imbalance, as evidenced by the altered metabolite trends, improved mitochondrial morphology, restored gene expression, and enhanced mitochondrial biosynthesis. Furthermore, DY131 enhanced the expression of TFAM, a mtDNA-binding protein which essential for mitochondrial genome and function maintenance [43].

AKI is characterized by a group of metabolic disorders and significant energy metabolic reprogramming was observed in renal tubular epithelial cells, subsequently resulting abnormality of metabolites [41]. Studies demonstrated that modulating the energy metabolism of renal tubular cells might serve as an effective strategy for AKI [56,57]. Altered metabolism of amino acid play a causal role in AKI progression. Renal proximal tubules reabsorb approximately 97–98% of filtered amino acids [58], while a remarkable loss of amino acid was observed in patients receiving renal replacement therapy with AKI an increased excretion of essential amino acids in AKI patients [59]. However, the regulation of most amino acid metabolic pathways and the therapeutic potential of targeting amino acid metabolism are less well understood. Our data showed significant alterations in metabolites in kidneys from cisplatin-treated mice, as other studies reported, and DY131 could recover the altered metabolism in kidneys. Besides, we also found that administration of DY131 alone *in vivo* induced significant changes in mitochondrial metabolism-related genes in kidneys, which are mainly enriched in mitochondrial respiratory chains and ATP synthesis (data were not shown). These findings confirmed the role of DY131 on regulating mitochondrial functions and metabolism. Furthermore, amino acid metabolic pathways were the most changed pathways after DY131 treatment, suggesting that DY131 might affect the regulation of amino acid metabolic pathways. Amino acids are essential for cell biological processes, and abnormal metabolism of amino acids might inhibit cell proliferation and induce cell apoptosis [60,61]. Impaired amino acid metabolism was observed in various types of AKI [62]. Amino acid supplementation is the mainly energy sources in normal kidney and was correlated with reduced AKI incidence [62,63]. Besides, clinical study showed that glycine level was elevated in patients with less severe AKI, suggesting its potential as a predictive biomarker for mortality of AKI [64]. Besides, administration of glycine has been demonstrated to protect renal epithelial cells in cisplatin-induced nephrotoxicity [65]. For serine and threonine, there were no studies for exploring their roles in AKI, which needs further investigation.

TFAM is a mitochondrial protein that functions in determining the abundance of the mitochondrial genome by regulating packaging, stability, and replication [66]. TFAM loss correlates with mtDNA damage in AKI patients and I/RI-induced AKI mice, resulting in decreased mitochondrial respiratory capacity and impaired mtDNA nucleoid

stability [67]. Our study demonstrated that DY131 treatment effectively reversed TFAM reduction in cisplatin-treated mice, accompanied by ERR γ 's capacity to up-regulate TFAM expression. Importantly, as predicted by JASPAR and further confirmed by *in vitro* experiments, we found that ERR γ could promote the transcription and expression of TFAM, suggesting a potential direct target of TFAM by ERR γ . Furthermore, a positive correlation between ERR γ and TFAM expression was found in human AKI datasets, which also supported our findings.

Of note, there are some limitations in our present study. First, our results demonstrated that ERR γ & DY131 protected against acute kidney injury *in vivo*, and DY131 could induce the transacted activity of ERR γ in renal tubular cells. However, this does not rule out that DY131 may play roles in ERR γ -independent manner. Further studies are needed to evaluate the effect of DY131 in renal tubular cell specific ERR γ knockout mice. Second, some reports indicated that DY131 displayed antitumor activity *in vivo*, but some other studies also indicated the opposite role of ERR γ in tumor pathogenesis [14,68,69]. Therefore, the effect of DY131 on tumor growth should be observed in the future studies. Third, the more detailed mechanism of DY131 and ERR γ on renal tubular cell metabolism need to be further explored.

Taken together, we found that DY131 promoted a renoprotective effect of ERR γ in various AKI murine models. Mechanistically, DY131 regulated ERR γ -TFAM axis to alleviate mitochondrial dysfunction, thereby regulating renal metabolism and resulting the improvement of renal tubular injury (Figure 8).

Conclusion

Our study demonstrated that ERR γ is closely associated with renal function in AKI and activation of ERR γ by its agonist DY131 protects renal function in different types of AKI. We also found that DY131 could ameliorate mitochondrial damage and metabolic disorders and promote TFAM expression, which might be a target gene of ERR γ . Our findings indicated that ERR γ agonist may represent a viable therapeutic strategy for improving renal metabolism and function in AKI.

Clinical perspectives

- The ERR γ , a member of orphan nuclear receptors which plays a regulatory role in many metabolic pathways was reduced in the kidney from AKI patients and animals with a negative correlation with AKI severity.
- DY131 activated ERR γ to improve mitochondrial function and renal metabolism through targeting TFAM.
- Targeting ERR γ through its agonist DY131 may be a potential therapeutic strategy to protect against AKI.

Data Availability

ERR γ protein expression in human kidneys were obtained from Human Protein Atlas. The public expression profiling by array was obtained from the genomics data repository Gene Expression Omnibus (GEO, NO. GSE1563), and the raw data of metabolomics in this study have been deposited to the metabolomics database Metabolomics Workbench (DatatrackID:4548).

Competing Interests

The authors declare that there are no competing interests associated with the manuscript.

Funding

This current work was supported by grants from the National Natural Science Foundation of China [grant numbers 81970581, 82170689, and 82170688]; Nanjing Medical Science and Technique Development Foundation [grant number JQX21008]; Social Development Fund of Jiangsu Province [grant number BE2021607]; “333” Talent Plan of Jiangsu province [grant numbers 333-2022001]; and National Key Research and Development Program [grant number 2019YFA0802702-1].

CRediT Author Contribution

Wei Gong: Conceptualization, Funding acquisition, Investigation, Visualization, Methodology, Writing—original draft, Writing—review & editing. **Lingling Lu:** Investigation, Visualization, Methodology, Writing—original draft, Writing—review & editing. **Haoyang Ma:** Validation, Investigation, Methodology. **Mingfeng Shan:** Validation, Investigation, Methodology. **Xinwen Fan:** Validation, Investigation, Methodology. **Mi Bai:** Funding acquisition, Investigation, Methodology. **Yue Zhang:** Conceptualization, Data curation, Writing—review & editing. **Songming Huang:** Conceptualization, Data curation, Funding acquisition, Writing—review & editing. **Zhanjun Jia:** Conceptualization, Data curation, Writing—review & editing. **Aihua Zhang:** Formal analysis, Supervision, Project administration, Writing—review & editing.

Abbreviations

AKI, acute kidney injury; BUN, blood urea nitrogen; CKD, chronic kidney disease; DEM, differentially expressed metabolite; ERRE, the ERR response element; ERR γ , estrogen-related receptor γ ; GEO, Gene Expression Omnibus; GFR, glomerular filtration rate; HPA, Human Protein Atlas; I/RI, ischemia/reperfusion injury; LPS, lipopolysaccharide; mtDNA, mitochondrial DNA; PCA, principal component analysis; Q-PCR, reverse transcription and quantitative real-time PCR; QC, quality control; rRNA, ribosomal RNA; RTECs, renal proximal tubular cells; Scr, creatinine; siRNA, small interfering RNA; TFAM, mitochondrial transcriptional factor A; VIP, variable importance in the projection.

References

- Turgut, F., Awad, A.S. and Abdel-Rahman, E.M. (2023) Acute kidney injury: medical causes and pathogenesis. *J. Clin. Med.* **12** (1), 375, <https://doi.org/10.3390/jcm12010375>
- Abebe, A., Kumela, K., Belay, M., Kebede, B. and Wobie, Y. (2021) Mortality and predictors of acute kidney injury in adults: a hospital-based prospective observational study. *Sci. Rep.* **11**, 15672, <https://doi.org/10.1038/s41598-021-94946-3>
- Harty, J. (2014) Prevention and management of acute kidney injury. *Ulster Med. J.* **83**, 149–157
- Kwiatkowska, E., Domanski, L., Dziedzic, V., Kajdy, A., Stefanska, K. and Kwiatkowski, S. (2021) The mechanism of drug nephrotoxicity and the methods for preventing kidney damage. *Int. J. Mol. Sci.* **22** (11), 6109, <https://doi.org/10.3390/ijms22116109>
- Fontecha-Barriuso, M., Lopez-Diaz, A.M., Guerrero-Mauvecin, J., Miguel, V., Ramos, A.M., Sanchez-Nino, M.D. et al. (2022) Tubular mitochondrial dysfunction, oxidative stress, and progression of chronic kidney disease. *Antioxidants (Basel)* **11** (7), 1356, <https://doi.org/10.3390/antiox11071356>
- van der Slikke, E.C., Star, B.S., van Meurs, M., Henning, R.H., Moser, J. and Bouma, H.R. (2021) Sepsis is associated with mitochondrial DNA damage and a reduced mitochondrial mass in the kidney of patients with sepsis-AKI. *Crit. Care* **25**, 36, <https://doi.org/10.1186/s13054-020-03424-1>
- Venkatachalam, M.A. and Weinberg, J.M. (2012) The tubule pathology of septic acute kidney injury: a neglected area of research comes of age. *Kidney Int.* **81**, 338–340, <https://doi.org/10.1038/ki.2011.401>
- Aki, T., Unuma, K. and Uemura, K. (2017) Emerging roles of mitochondria and autophagy in liver injury during sepsis. *Cell Stress* **1**, 79–89, <https://doi.org/10.15698/cst2017.11.110>
- Oh, C.J., Kim, M.J., Lee, J.M., Kim, D.H., Kim, I.Y., Park, S. et al. (2023) Inhibition of pyruvate dehydrogenase kinase 4 ameliorates kidney ischemia-reperfusion injury by reducing succinate accumulation during ischemia and preserving mitochondrial function during reperfusion. *Kidney Int.* **104**, 724–739, <https://doi.org/10.1016/j.kint.2023.06.022>
- Lu, Q., Wang, M., Gui, Y., Hou, Q., Gu, M., Liang, Y. et al. (2020) Rheb1 protects against cisplatin-induced tubular cell death and acute kidney injury via maintaining mitochondrial homeostasis. *Cell Death Dis.* **11**, 364, <https://doi.org/10.1038/s41419-020-2539-4>
- Ariazi, E.A., Clark, G.M. and Mertz, J.E. (2002) Estrogen-related receptor alpha and estrogen-related receptor gamma associate with unfavorable and favorable biomarkers, respectively, in human breast cancer. *Cancer Res.* **62**, 6510–6518
- Heard, D.J., Norby, P.L., Holloway, J. and Vissing, H. (2000) Human ERRgamma, a third member of the estrogen receptor-related receptor (ERR) subfamily of orphan nuclear receptors: tissue-specific isoforms are expressed during development and in the adult. *Mol. Endocrinol.* **14**, 382–392
- Yu, S., Wang, X., Ng, C.F., Chen, S. and Chan, F.L. (2007) ERRgamma suppresses cell proliferation and tumor growth of androgen-sensitive and androgen-insensitive prostate cancer cells and its implication as a therapeutic target for prostate cancer. *Cancer Res.* **67**, 4904–4914, <https://doi.org/10.1158/0008-5472.CAN-06-3855>
- Kim, J.H., Choi, Y.K., Byun, J.K., Kim, M.K., Kang, Y.N., Kim, S.H. et al. (2016) Estrogen-related receptor gamma is upregulated in liver cancer and its inhibition suppresses liver cancer cell proliferation via induction of p21 and p27. *Exp. Mol. Med.* **48**, e213, <https://doi.org/10.1038/emmm.2015.115>
- Sanyal, S., Kim, J.Y., Kim, H.J., Takeda, J., Lee, Y.K., Moore, D.D. et al. (2002) Differential regulation of the orphan nuclear receptor small heterodimer partner (SHP) gene promoter by orphan nuclear receptor ERR isoforms. *J. Biol. Chem.* **277**, 1739–1748, <https://doi.org/10.1074/jbc.M106140200>
- Shirakawa, J. and Kulkarni, R.N. (2016) ERRgamma—a new player in beta cell maturation. *Cell Metab.* **23**, 765–767, <https://doi.org/10.1016/j.cmet.2016.04.026>
- Misra, J., Kim, D.K. and Choi, H.S. (2017) ERRgamma: a junior orphan with a senior role in metabolism. *Trends Endocrinol. Metab.* **28**, 261–272, <https://doi.org/10.1016/j.tem.2016.12.005>
- Sopariwala, D.H., Rios, A.S., Saley, A., Kumar, A. and Narkar, V.A. (2023) Estrogen-related receptor gamma gene therapy promotes therapeutic angiogenesis and muscle recovery in preclinical model of PAD. *J. Am. Heart Assoc.* **12**, e028880, <https://doi.org/10.1161/JAHA.122.028880>
- Pei, L., Mu, Y., Leblanc, M., Alaynick, W., Barish, G.D., Pankratz, M. et al. (2015) Dependence of hippocampal function on ERRgamma-regulated mitochondrial metabolism. *Cell Metab.* **21**, 628–636, <https://doi.org/10.1016/j.cmet.2015.03.004>

- 20 Flechner, S.M., Kurian, S.M., Head, S.R., Sharp, S.M., Whisenant, T.C., Zhang, J. et al. (2004) Kidney Transplant rejection and tissue injury by gene profiling of biopsies and peripheral blood lymphocytes. [Available from: <https://www.ncbi.nlm.nih.gov/geo/query/acc.cgi?acc=GSE1563>, <https://doi.org/10.1111/j.1600-6143.2004.00526.x>
- 21 Flechner, S.M., Kurian, S.M., Head, S.R., Sharp, S.M., Whisenant, T.C., Zhang, J. et al. (2004) Kidney transplant rejection and tissue injury by gene profiling of biopsies and peripheral blood lymphocytes. *Am. J. Transplant.* **4**, 1475–1489, <https://doi.org/10.1111/j.1600-6143.2004.00526.x>
- 22 Shi, L., Zha, H., Pan, Z., Wang, J., Xia, Y., Li, H. et al. (2023) DUSP1 protects against ischemic acute kidney injury through stabilizing mtDNA via interaction with JNK. *Cell Death Dis.* **14**, 724, <https://doi.org/10.1038/s41419-023-06247-4>
- 23 Yang, Y., Liu, S., Wang, P., Ouyang, J., Zhou, N., Zhang, Y. et al. (2023) DNA-dependent protein kinase catalytic subunit (DNA-PKcs) drives chronic kidney disease progression in male mice. *Nat. Commun.* **14**, 1334, <https://doi.org/10.1038/s41467-023-37043-5>
- 24 Wu, M., Jin, Q., Xu, X., Fan, J., Chen, W., Miao, M. et al. (2023) TP53RK Drives the progression of chronic kidney disease by phosphorylating Birc5. *Adv. Sci. (Weinh)* **10**, e2301753, <https://doi.org/10.1002/adv.202301753>
- 25 Peng, W., Zhou, X., Xu, T., Mao, Y., Zhang, X., Liu, H. et al. (2022) BMP-7 ameliorates partial epithelial-mesenchymal transition by restoring SnoN protein level via Smad1/5 pathway in diabetic kidney disease. *Cell Death Dis.* **13**, 254, <https://doi.org/10.1038/s41419-022-04529-x>
- 26 Gong, W., Lu, L., Zhou, Y., Liu, J., Ma, H., Fu, L. et al. (2021) The novel STING antagonist H151 ameliorates cisplatin-induced acute kidney injury and mitochondrial dysfunction. *Am. J. Physiol. Renal. Physiol.* **320**, F608–F616, <https://doi.org/10.1152/ajprenal.00554.2020>
- 27 Ma, H., Liu, J., Du, Y., Zhang, S., Cao, W., Jia, Z. et al. (2021) Estrogen-related receptor gamma agonist DY131 ameliorates lipopolysaccharide-induced acute liver injury. *Front Pharmacol.* **12**, 626166, <https://doi.org/10.3389/fphar.2021.626166>
- 28 Lu, L., Liu, W., Li, S., Bai, M., Zhou, Y., Jiang, Z. et al. (2023) Flavonoid derivative DMXAA attenuates cisplatin-induced acute kidney injury independent of STING signaling. *Clin. Sci. (Lond.)* **137**, 435–452, <https://doi.org/10.1042/CS20220728>
- 29 Zhao, S.L., Wei, S.Y., Wang, Y.X., Diao, T.T., Li, J.S., He, Y.X. et al. (2016) Wnt4 is a novel biomarker for the early detection of kidney tubular injury after ischemia/reperfusion injury. *Sci. Rep.* **6**, 32610, <https://doi.org/10.1038/srep32610>
- 30 Xu, Y., Qin, S., Niu, Y., Gong, T., Zhang, Z. and Fu, Y. (2020) Effect of fluid shear stress on the internalization of kidney-targeted delivery systems in renal tubular epithelial cells. *Acta Pharm. Sin. B.* **10**, 680–692, <https://doi.org/10.1016/j.apsb.2019.11.012>
- 31 Gong, W., Song, J., Liang, J., Ma, H., Wu, W., Zhang, Y. et al. (2021) Reduced Lon protease 1 expression in podocytes contributes to the pathogenesis of podocytopathy. *Kidney Int.* **99**, 854–869, <https://doi.org/10.1016/j.kint.2020.10.025>
- 32 Chen, L., Ding, H., Zhu, Y., Guo, Y., Tang, Y., Xie, K. et al. (2023) Untargeted and targeted metabolomics identify metabolite biomarkers for Salmonella enteritidis in chicken meat. *Food Chem.* **409**, 135294, <https://doi.org/10.1016/j.foodchem.2022.135294>
- 33 Lingling, L. (2024) The metabolomic resetting effect of DY131 in cisplatin-induced AKI. [updated 2023.12.21. Available from: <http://dev.metabolomicsworkbench.org:22222/data/DRCCMetadata.php?Mode=Study&StudyID=ST003042&Access=VslG8026>
- 34 Soni, S.S., Cruz, D., Bobek, I., Chionh, C.Y., Nalesso, F., Lentini, P. et al. (2010) NGAL: a biomarker of acute kidney injury and other systemic conditions. *Int. Urol. Nephrol.* **42**, 141–150, <https://doi.org/10.1007/s11255-009-9608-z>
- 35 (2024) Tissue expression of ESRG-Staining in kidney-The Human Protein Atlas. Available from: <https://www.proteinatlas.org/ENSG00000196482-ESRRG/tissue/kidney>
- 36 Chang, H., Hanawa, H., Liu, H., Yoshida, T., Hayashi, M., Watanabe, R. et al. (2006) Hydrodynamic-based delivery of an interleukin-22-Ig fusion gene ameliorates experimental autoimmune myocarditis in rats. *J. Immunol.* **177**, 3635–3643, <https://doi.org/10.4049/jimmunol.177.6.3635>
- 37 Wang, Z., Xiao, H., Dong, J., Li, Y., Wang, B., Chen, Z. et al. (2023) Sexual dimorphism in gut microbiota dictates therapeutic efficacy of intravenous immunoglobulin on radiotherapy complications. *J. Adv. Res.* **46**, 123–133, <https://doi.org/10.1016/j.jare.2022.06.002>
- 38 Yu, D.D. and Forman, B.M. (2005) Identification of an agonist ligand for estrogen-related receptors ERbeta/gamma. *Bioorg. Med. Chem. Lett.* **15**, 1311–1313, <https://doi.org/10.1016/j.bmcl.2005.01.025>
- 39 Huppunen, J., Wohlfahrt, G. and Aarnisalo, P. (2004) Requirements for transcriptional regulation by the orphan nuclear receptor ERRgamma. *Mol. Cell. Endocrinol.* **219**, 151–160, <https://doi.org/10.1016/j.mce.2004.01.002>
- 40 Heckler, M.M., Thakor, H., Schafer, C.C. and Riggins, R.B. (2014) ERK/MAPK regulates ERRgamma expression, transcriptional activity and receptor-mediated tamoxifen resistance in ER+ breast cancer. *FEBS J.* **281**, 2431–2442, <https://doi.org/10.1111/febs.12797>
- 41 Li, Y., Hepokoski, M., Gu, W., Simonson, T. and Singh, P. (2021) Targeting mitochondria and metabolism in acute kidney injury. *J. Clin. Med.* **10** (17), 3991, <https://doi.org/10.3390/jcm10173991>
- 42 Tang, C., Cai, J., Yin, X.M., Weinberg, J.M., Venkatachalam, M.A. and Dong, Z. (2021) Mitochondrial quality control in kidney injury and repair. *Nat. Rev. Nephrol.* **17**, 299–318, <https://doi.org/10.1038/s41581-020-00369-0>
- 43 Guo, Y., Ni, J., Chen, S., Bai, M., Lin, J., Ding, G. et al. (2018) MicroRNA-709 mediates acute tubular injury through effects on mitochondrial function. *J. Am. Soc. Nephrol.* **29**, 449–461, <https://doi.org/10.1681/ASN.2017040381>
- 44 Rauluseviciute, I., Riudavets-Puig, R., Blanc-Mathieu, R., Castro-Mondragon, J.A., Ferenc, K., Kumar, V. et al. (2024) JASPAR 2024: 20th anniversary of the open-access database of transcription factor binding profiles. *Nucleic Acids Res.* **52**, D174–D182, <https://doi.org/10.1093/nar/gkad1059>
- 45 Giulivi, C., Zhang, K. and Arakawa, H. (2023) Recent advances and new perspectives in mitochondrial dysfunction. *Sci. Rep.* **13**, 7977, <https://doi.org/10.1038/s41598-023-34624-8>
- 46 Vringer, E. and Tait, S.W.G. (2023) Mitochondria and cell death-associated inflammation. *Cell Death Differ.* **30**, 304–312, <https://doi.org/10.1038/s41418-022-01094-w>
- 47 Fagerberg, L., Hallstrom, B.M., Oksvold, P., Kampf, C., Djureinovic, D., Odeberg, J. et al. (2014) Analysis of the human tissue-specific expression by genome-wide integration of transcriptomics and antibody-based proteomics. *Mol. Cell. Proteomics* **13**, 397–406, <https://doi.org/10.1074/mcp.M113.035600>
- 48 Yoshihara, E., Wei, Z., Lin, C.S., Fang, S., Ahmadian, M., Kida, Y. et al. (2016) ERRgamma is required for the metabolic maturation of therapeutically functional glucose-responsive beta cells. *Cell Metab.* **23**, 622–634, <https://doi.org/10.1016/j.cmet.2016.03.005>

- 49 Fan, W., He, N., Lin, C.S., Wei, Z., Hah, N., Waizenegger, W. et al. (2018) ERRgamma promotes angiogenesis, mitochondrial biogenesis, and oxidative remodeling in PGC1alpha/beta-deficient muscle. *Cell Rep.* **22**, 2521–2529, <https://doi.org/10.1016/j.celrep.2018.02.047>
- 50 Zhao, J., Lupino, K., Wilkins, B.J., Qiu, C., Liu, J., Omura, Y. et al. (2018) Genomic integration of ERRgamma-HNF1beta regulates renal bioenergetics and prevents chronic kidney disease. *Proc. Natl. Acad. Sci. U.S.A.* **115**, E4910–E4919, <https://doi.org/10.1073/pnas.1804965115>
- 51 Audet-Walsh, E., Yee, T., McGuirk, S., Vernier, M., Ouellet, C., St-Pierre, J. et al. (2017) Androgen-dependent repression of ERRgamma reprograms metabolism in prostate cancer. *Cancer Res.* **77**, 378–389, <https://doi.org/10.1158/0008-5472.CAN-16-1204>
- 52 Misra, J., Kim, D.K. and Choi, H.S. (2017) ERRγ: a junior orphan with a senior role in metabolism. *Trends Endocrinol. Metab.* **28**, 261–272, <https://doi.org/10.1016/j.tem.2016.12.005>
- 53 Choi, J., Oh, T.G., Jung, H.W., Park, K.Y., Shin, H., Jo, T. et al. (2022) Estrogen-related receptor gamma maintains pancreatic acinar cell function and identity by regulating cellular metabolism. *Gastroenterology* **163**, 239–256, <https://doi.org/10.1053/j.gastro.2022.04.013>
- 54 Kim, H.J., Kim, B.K., Ohk, B., Yoon, H.J., Kang, W.Y., Cho, S. et al. (2019) Estrogen-related receptor gamma negatively regulates osteoclastogenesis and protects against inflammatory bone loss. *J. Cell. Physiol.* **234**, 1659–1670, <https://doi.org/10.1002/jcp.27035>
- 55 Zou, Z., Harris, L.K., Forbes, K. and Heazell, A.E.P. (2022) Placental expression of estrogen-related receptor gamma is reduced in fetal growth restriction pregnancies and is mediated by hypoxiadder. *Biol. Reprod.* **107**, 846–857, <https://doi.org/10.1093/biolre/iuac108>
- 56 Tanuseputero, S.A., Lin, M.T., Yeh, S.L. and Yeh, C.L. (2020) Intravenous arginine administration downregulates NLRP3 inflammasome activity and attenuates acute kidney injury in mice with polymicrobial sepsis. *Mediators Inflamm.* **2020**, 3201635, <https://doi.org/10.1155/2020/3201635>
- 57 Andrianova, N.V., Buyan, M.I., Bolikhova, A.K., Zorov, D.B. and Plotnikov, E.Y. (2021) Dietary restriction for kidney protection: decline in nephroprotective mechanisms during aging. *Front Physiol.* **12**, 699490, <https://doi.org/10.3389/fphys.2021.699490>
- 58 Garibotto, G., Sofia, A., Saffioti, S., Bonanni, A., Mannucci, I. and Verzola, D. (2010) Amino acid and protein metabolism in the human kidney and in patients with chronic kidney disease. *Clin. Nutr.* **29**, 424–433, <https://doi.org/10.1016/j.clnu.2010.02.005>
- 59 Oh, W.C., Mafrici, B., Rigby, M., Harvey, D., Sharman, A., Allen, J.C. et al. (2019) Micronutrient and amino acid losses during renal replacement therapy for acute kidney injury. *Kidney Int. Rep.* **4**, 1094–1108, <https://doi.org/10.1016/j.ekir.2019.05.001>
- 60 Wang, Z., Zhao, F., Xu, C., Zhang, Q., Ren, H., Huang, X. et al. (2024) Metabolic reprogramming in skin wound healing. *Burns Trauma.* **12**, tkad047, <https://doi.org/10.1093/burnst/tkad047>
- 61 Assi, G. and Faour, W.H. (2023) Arginine deprivation as a treatment approach targeting cancer cell metabolism and survival: A review of the literature. *Eur. J. Pharmacol.* **953**, 175830, <https://doi.org/10.1016/j.ejphar.2023.175830>
- 62 Tang, W. and Wei, Q. (2023) The metabolic pathway regulation in kidney injury and repair. *Front Physiol.* **14**, 1344271, <https://doi.org/10.3389/fphys.2023.1344271>
- 63 Kazawa, M., Kabata, D., Yoshida, H., Minami, K., Maeda, T., Yoshitani, K. et al. (2024) Amino acids to prevent cardiac surgery-associated acute kidney injury: a randomized controlled trial. *JA Clin. Rep.* **10**, 19, <https://doi.org/10.1186/s40981-024-00703-6>
- 64 Gisewhite, S., Stewart, I.J., Beilman, G. and Luszczek, E. (2021) Urinary metabolites predict mortality or need for renal replacement therapy after combat injury. *Crit. Care* **25**, 119, <https://doi.org/10.1186/s13054-021-03544-2>
- 65 Heyman, S.N., Rosen, S., Silva, P., Spokes, K., Egorin, M.J. and Epstein, F.H. (1991) Protective action of glycine in cisplatin nephrotoxicity. *Kidney Int.* **40**, 273–279, <https://doi.org/10.1038/ki.1991.210>
- 66 Kang, I., Chu, C.T. and Kaufman, B.A. (2018) The mitochondrial transcription factor TFAM in neurodegeneration: emerging evidence and mechanisms. *FEBS Lett.* **592**, 793–811, <https://doi.org/10.1002/1873-3468.12989>
- 67 Zhao, M., Wang, Y., Li, L., Liu, S., Wang, C., Yuan, Y. et al. (2021) Mitochondrial ROS promote mitochondrial dysfunction and inflammation in ischemic acute kidney injury by disrupting TFAM-mediated mtDNA maintenance. *Theranostics* **11**, 1845–1863, <https://doi.org/10.7150/thno.50905>
- 68 Huang, B., Mu, P., Yu, Y., Zhu, W., Jiang, T., Deng, R. et al. (2021) Inhibition of EZH2 and activation of ERRgamma synergistically suppresses gastric cancer by inhibiting FOXM1 signaling pathway. *Gastric Cancer* **24**, 72–84, <https://doi.org/10.1007/s10120-020-01097-x>
- 69 Kim, J., Hwang, H., Yoon, H., Lee, J.E., Oh, J.M., An, H. et al. (2020) An orally available inverse agonist of estrogen-related receptor gamma showed expanded efficacy for the radioiodine therapy of poorly differentiated thyroid cancer. *Eur. J. Med. Chem.* **205**, 112501, <https://doi.org/10.1016/j.ejmech.2020.112501>